A Preliminary Study of Handprint Synthesis

Jianjiang Feng, Huapeng Zhou, and Jie Zhou

Department of Automation
Tsinghua University, Beijing, China
{jfeng,jzhou}@tsinghua.edu.cn

Abstract. Handprint, the friction ridge pattern on human hand, is of vital importance for recognizing repeat offenders and suspects in forensics. In this paper, we proposed a set of statistical models for the main features in whole handprints, including hand contour, major creases, and ridge patterns. Based on these statistical models, a handprint synthesis algorithm is proposed, which is useful for technology evaluation due to the lack of high resolution handprint databases in the public domain.

Keywords: Texture synthesis, fingerprint, palmprint, singularity.

1 Introduction

For over one hundred years, handprints (see Fig. 1a) have been routinely used by law enforcement agencies throughout the world to identify suspects and victims [1]. Without question, among all the regions of hands, ridge pattern on fingertips has the highest practical value and has received the most attention. In fact, only fingerprints have found wide application in non-forensic areas. However, recognition solely based on fingertips has some inherent problems when fingerprints are of poor quality, unreliable or unavailable. For example, fingerprints of elderly people and manual workers are often flattened and contain many creases or cuts, criminals may surgically alter their fingerprints to avoid being recognized by fingerprint recognition systems, and latent prints lifted from crime scenes may have been left by lower finger segments or palms.

To deal with these problems, a very nature solution is to extend ridge pattern recognition from fingerprints to whole handprints. However, simply applying fingerprint analysis and matching techniques to the whole handprints is not very effective, due to the differences between different regions of handprints. Significant research efforts should be devoted to lower finger segments and the palm, which have received very little attention in the past.

In this paper, we study the probability distributions of main features in handprints, including hand contour, major creases, and singular points. Statistical models of handprints have potential values for a number of problems in handprint recognition, including feature extraction, matching, indexing, and synthesis. Although several researchers have studied the probability distributions of some of the features in handprints, such as hand contour [2] and singularity in fingerprints [3], our statistical model is more comprehensive, covering three main

Z. Sun et al. (Eds.): CCBR 2011, LNCS 7098, pp. 133–140, 2011.

features in all regions of handprints and considering the correlation between different features and between different regions.

We also applied the proposed statistical model to handprint synthesis. Handprint synthesis technique is very desirable because the lack of public domain high resolution handprint databases has hindered the research on handprint recognition. Although there exists some researches that can synthesize some of features or regions of handprints, such as hand shape synthesis [2], low resolution palmprint synthesis [4], and fingerprint synthesis [5], synthesis of high resolution full handprint images has not yet been addressed.

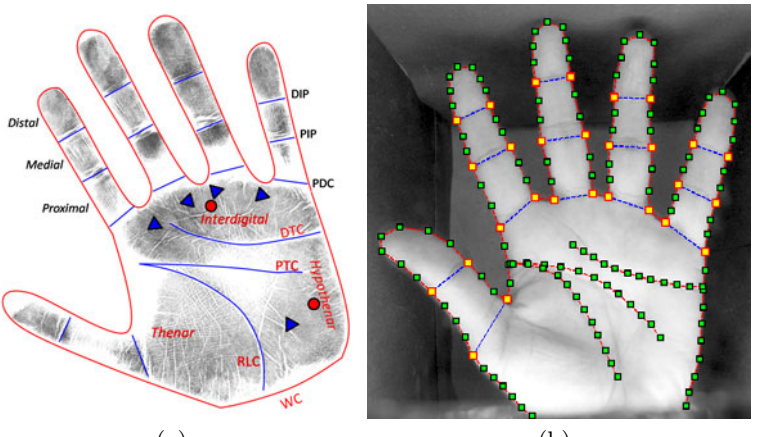

(a) (b)

Fig. 1. (a) A high resolution handprint obtained using ink-on-paper method. Hand contour, major creases, and singular points (loop and delta) are marked. (b) A low resolution handprint and manually marked lankmark points.

2 Statistical Modeling

2.1 Terms

The human hand consists of the palm and five fingers. Both the finger and the palm are divided into regions by permanent flexion creases, which are wide white lines in the handprint image in Fig. 1a. The finger consists of three parts: the distal segment, the medial segment, and the proximal segment, which are separated by the distal interphalangeal crease (DIP), the proximal interphalangeal crease (PIP), and the proximal digital crease (PDC). The palm can be further divided into three areas: interdigital, thenar, and hypothenar, by three major palm flexion creases: radial longitudinal crease (RLC), proximal transverse crease (PTC), and distal transverse crease (DTC). The wrist crease (WC) defines the boundary between the palm and the arm.

2.2 Contour and Creases

Since both hand contour and major palmar creases have regular structure, we employ a statistical shape model [2] to model these two features. By modeling contours and major palmar creases together, we can take into account the correlation between these features and avoid generating invalid handprints. Phalangeal creases are assumed to be straight lines between corresponding landmark points on hand contour.

The first step in statistical shape modeling is to label the training set. As we do not have a large database of high resolution handprint images like the image in Fig. 1a, IIT Delhi Touchless Palmprint Database (`http://web.iitd.ac.in/~ajaykr/Database_Palm.htm`), was used to study the interclass variations of hand contours and major palmar creases. Landmark points of 100 different left hands were manually marked by the authors. The hand contour is represented by 118 landmark points, while each of the three major palmal creases is defined by 12 points uniformly distributed on the crease. Figure 1b shows the annotated landmark points on a low resolution handprint image. The algorithm described in [2] is then used to learn the statistics of these points in the training set.

2.3 Ridge Pattern

Handprint identification in forensics is exclusively based on matching ridge patterns. Thus modeling the ridge patterns on hands is of crucial importance in modeling handprints. Inspired by the method in [5], a ridge pattern $\mathbf{r}$ is viewed as the result of performing iterative contextual filtering, governed by ridge orientation field $\mathbf{o}$ and ridge frequency map $\mathbf{f}$, on a random noise image $\mathbf{n}$. It is defined as $\mathbf{r} = \mathit{Filtering}(\mathbf{n}, \mathbf{o}, \mathbf{f})$. In other words, a ridge pattern $\mathbf{r}$ is a deterministic transformation of three random vectors: noise image $\mathbf{n}$, orientation field $\mathbf{o}$, and frequency map $\mathbf{f}$. The function $\mathit{Filtering}()$ represents the iterative Gabor filtering. The role of the noise image $\mathbf{n}$ is to support the variability of ridge patterns with the same orientation field and frequency map. We determined that an i.i.d. uniform distribution model in the range $[0, 1]$ is suitable for the noise image. Since the variability of ridge frequency map $\mathbf{f}$ is not large, we assume a fixed ridge frequency (0.1 ridges per pixel) for ridge patterns and focus on studying the probability distribution of orientation field $\mathbf{o}$ in this work.

2.4 Orientation Field

We have observed that ridge orientation field on the hand is quite consistent with major creases except for the singularity region. Thus, we model an orientation field $\mathbf{o}$ as $\mathbf{o} = \mathit{Reconstruct}(\mathbf{c}, \mathbf{s})$, namely a deterministic transformation of two random vectors: creases $\mathbf{c}$ and singular points $\mathbf{s}$. Statistical modeling of major creases has already been covered in Sec. 2.2. Statistical modeling of singularity will be discussed in the next subsection. Here we describe how orientation field is reconstructed based on creases and singularity.

Orientation field is reconstructed separately for the palm and each segment of each finger. When reconstructing orientation field for a specific region, only the boundary creases of that region and the singular points in that region are used. The boundaries of the distal segment of finger include the hand contour around the fingertip and the distal interphalangeal crease. The boundaries of the medial segment and the proximal segment of finger includes the three phalangeal creases. The boundaries of the palm contain the proximal interphalangeal creases of five fingers, the wrist crease, and three major palm creases.

Given the singular points (if present), the boundary creases (each represented as an ordered set of sampling points), and the region of interest, the proposed orientation field reconstruction algorithm consists of five steps (see the flowchart in Fig. 2):

1. For each line segment between two consecutive sampling points on each boundary crease, the orientation of the line segment is used as the local ridge orientation at all the blocks passed by the line segment. A sparse orientation field, called boundary orientation field, is generated after this step.
2. The singular orientation field is computed by the Zero-Pole model [6].
3. The singular orientation field is subtracted from the boundary orientation field to obtain the boundary continuous orientation field.
4. A bivariate polynomial model is fitted to the boundary continuous orientation field and used to predict the whole continuous orientation field.
5. The final orientation field is obtained by adding the singular orientation field to the continuous orientation field.

Steps 3 and 5 can be omitted if there are no singular points, for example, in arch-type fingerprints. Note that the same algorithm is used for each region of the hand. The order of polynomial model is three for the palm and two for the finger region.

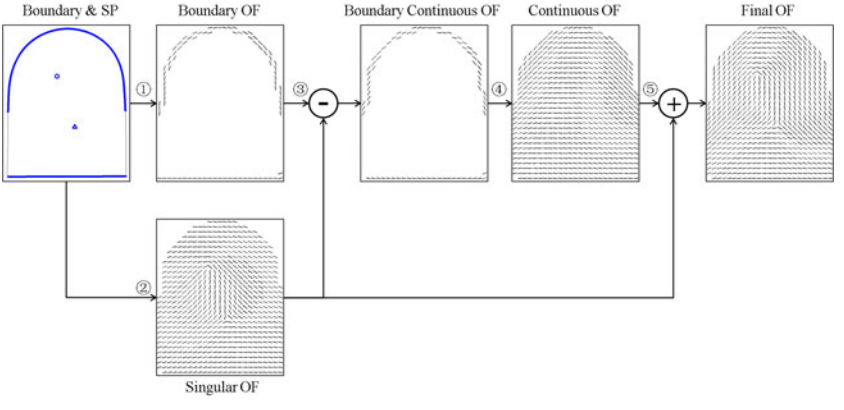

Fig. 2. Orientation field (OF) reconstruction from finger boundary and a pair of singular points (SP)

2.5 Singularity Configuration

A singularity configuration is a set of singularities $s = \{(x_1, y_1, t_1), \cdots, (x_n, y_n, t_n)\}$, where n is the number of singularities, x_i and y_i are the location of the ith singularity, and t_i is the type of the ith singularity. For a loop-type singularity, $t_i = 1$. For a delta-type singularity, $t_i = -1$. Both the number n and the location of singularities are random variables. As the statistical modeling of a random set of points is not convenient, we categorize all possible singularity configurations on the hand into several types according to the number of loops and deltas. In each type of configuration, a fixed order is defined for the singularities. In this way, we only need to study the probability distributions of the locations of singularity of each type of configuration, which is a random vector, $s_t = (x_1, y_1, \cdots, x_{t_n}, y_{t_n})$, where t_n denotes the number of singular points in the configuration of type t.

To reduce the dimensionality of the singularity vector, we chose to study the distribution of singularity configurations in different regions separately. We have observed that singular points generally appear only on the distal segment of the fingers, and the interdigital and hypothenar region of the palm. Since the singular points in these regions are far from each other, we assume that they are independent of each other and study the probability distributions of singularity vectors in each region separately. The number of singular points in a simply-connected region satisfies the Penrose formula [7]: $(N_L - N_D) \cdot \pi = \theta$, where θ denotes the cumulative orientation change along the boundary of the region, and N_L and N_D denote the numbers of loops and deltas inside the region, respectively. For this reason, there are only a small number of feasible singularity configurations in fingers and palms. The details of singularity configurations in three regions are given below.

Distal Segment of Finger. Since the cumulative orientation change along the boundary of a complete fingerprint is always zero, $N_L = N_D$ holds for all fingerprints. Since the probability that a fingerprint contains more than two loops is very rare, we can categorize singularity configurations on fingerprints into three major types: no singularity, one pair of loop and delta points, and two pairs of loop and delta points. The order of singular points is fixed for each of the two types of configurations. In the case of one pair of loop and delta points, the order of singular points is loop and then delta. In the case of two pairs of loop and delta points, the order is top loop, bottom loop, left delta, and then right delta.

The distribution of singularity on fingerprints has been quantitatively studied by Cappelli and Maltoni [3]. But the method used here has two differences from [3]. The first difference is that we use the distal interphalangeal crease as the x axis and the center point of the crease as the origin. This coordinate system is more robust than the coordinate system in [3], which is based on the left and right boundaries of fingerprints and the centroid of fingerprints. The second difference is that we unify ulnar loop, radial loop, and tented arch into one type, since a finer classification is ambiguous in some situations. Singular points and

creases of 200 plain fingerprints in NIST SD29 were manually marked and the p.d.f. of two types of singularity vectors are estimated with a Gaussian mixture model.

Interdigital Region. The number of loops, N_L, and the number of deltas, N_D, in the interdigital region satisfy the formula $N_D - N_L = 3$. We noticed that two types of singularity configurations are very common in our palmprint database, which is provided by a law enforcement agency. The most common type consists of four deltas, each associated with a finger, and one loop. The second most common type consists of five deltas and two loops. Other types of configurations are not considered now since sufficient data is not available for estimating their probability distribution. The order of singular points is fixed for each of the two types of configurations. In the first type of configuration, the order is the loop, and then the four delta points sorted along the ulnar direction (from little to ring finger). In the second type of configuration, the order is the two loop points sorted along the ulnar direction, four delta points associated with fingers sorted along the ulnar direction, followed by the additional delta.

The top endpoint of crease PTC and the bottom endpoint of crease DTC are used as reference points to register palmprints. Singular points and reference points of 2,000 palmprints in our database were manually marked for studying the distribution of singularity on the palm. Gaussian mixture models are used to estimate the p.d.f. of the two types of singularity configurations.

Hypothenar Region. The number of loops, N_L, and the number of deltas, N_D, in the interdigital region satisfy the formula $N_D - N_L = 1$. The most common singularity configuration consists of only one delta, the so-called carpal delta, which is generally located between thenar and hypothenar and just above the wrist crease. The second most common type consists of two deltas and one loop. Other types of configurations are not considered since sufficient data is not available for estimating their probability distribution. The order of singular points is fixed for each of the two types of configurations. In the second type of configuration, the order is the loop followed by the two delta points sorted from top to bottom. Gaussian mixture models are used to estimate the p.d.f. of the two types of singularity configurations.

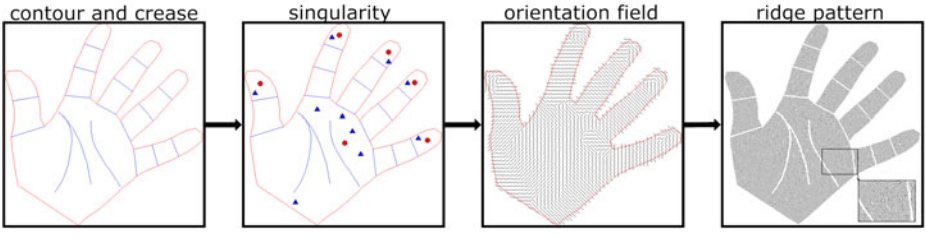

Fig. 3. Flowchart of the proposed handprint synthesis algorithm

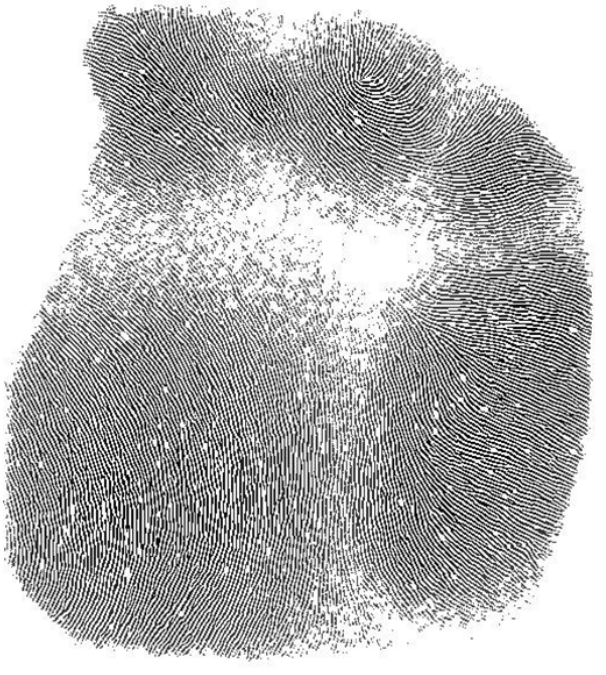

Fig. 4. Palm region of a synthesized handprint with noise added

3 Synthesis

With the statistical models described in the preceding sections, we generate a handprint image through the following four steps (see the flowchart in Fig. 3):

1. Contour and major crease generation. Landmark points on hand contour and major palmar creases are generated by sampling their statistical model. Hand contour and palmar creases are obtained by connecting landmark points. Phalangeal creases are generated by connecting the corresponding landmark points on the hand contour.
2. Singular point generation. Singular points are generated for each finger and the palm region separately. The first step is to sample the singularity configuration. The second step is to generate a random vector according to the statistical model of the selected configuration. The last step is to transform the singularities using the finger or palm coordinate system.
3. Orientation field reconstruction. For each finger segment and the palm, orientation field is reconstructed using the singular points in the region and the boundary.
4. Ridge pattern generation. Ridge pattern is generated by performing iterative Gabor filtering (5 iterations) on a randomly seeded image. Finally, major creases are drawn on the ridge pattern as wide white lines.

The synthesized handprint can be made more realistic by adding noise using the method of SFinGe [5]. See Fig. 4 for the palm area of a synthesized handprint with noise added.

4 Summary and Future Directions

Fingerprint recognition systems do not function well when fingerprints are of poor quality or not available. A natural solution to overcome these problems is to develop recognition systems to utilize the entire handprint. To understand the handprints, we have conducted a comprehensive study on the probability distribution of the main features in handprints, including hand contour, major creases, and ridge pattern. For different features, appropriate statistical models are proposed and estimated using large databases of training images. Based on these statistical models, we have proposed a handprint synthesis algorithm that can generate high resolution synthetic handprint images.

To generate more realistic handprint images, we need to model the probability distribution of minor creases and the intraclass variations in several aspects, such as contact area, distortion, brightness, contrast, and ridge width. We will also conduct experiments to see whether the performance of handprint recognition algorithms on synthesized handprint datasets is consistent with their performance on real handprint datasets.

Acknowledgments. This work was supported by the National Natural Science Foundation of China under Grants 61020106004, 60875017, 61005023, and 61021063.

References

1. Maltoni, D., Maio, D., Jain, A.K., Prabhakar, S.: Handbook of Fingerprint Recognition. Springer, Heidelberg (2003)
2. Cootes, T.F., Taylor, C.J., Cooper, D.H.: Active Shape Models—Their Training and Application. CVIU 61(1), 38–59 (1995)
3. Cappelli, R., Maltoni, D.: On the Spatial Distribution of Fingerprint Singularities. IEEE Trans. on PAMI. 31(4), 742–748 (2009)
4. Wei, Z., Han, Y., Sun, Z., Tan, T.: Palmprint Image Synthesis: A Preliminary Study. In: ICIP, pp. 285–288 (2008)
5. Cappelli, R., Maio, D., Maltoni, D.: Synthetic Fingerprint-Database Generation. In: ICPR, pp. 744–747 (2002)
6. Sherlock, B.G., Monro, D.M.: A Model for Interpreting Fingerprint Topology. Pattern Recognition 26(7), 1047–1055 (1993)
7. Penrose, R.: The Topology of Ridge Systems. Annals of Human Genetics 42(4), 435–444 (1979)